HHS Public Access

Author manuscript

Nature. Author manuscript; available in PMC 2018 April 09.

Published in final edited form as:

Nature. 2017 October 05; 550(7674): 133–136. doi:10.1038/nature24040.

PAK Signaling Drives Acquired Drug Resistance to MAPK Inhibitors in *BRAF*-mutant Melanomas

Hezhe Lu[1,15], **Shujing Liu**[2,15], **Gao Zhang**[3,15], **Bin Wu**[1], **Yueyao Zhu**[1], **Dennie T. Frederick**[4], **Yi Hu**[5], **Wenqun Zhong**[1], **Sergio Randell**[3], **Norah Sadek**[3], **Wei Zhang**[1], **Gang Chen**[1], **Chaoran Cheng**[6], **Jingwen Zeng**[1], **Lawrence W. Wu**[3], **Jie Zhang**[6], **Xiaoming Liu**[2], **Wei Xu**[7], **Clemens Krepler**[3], **Katrin Sproesser**[3], **Min Xiao**[3], **Benchun Miao**[4], **Jianglan Liu**[3], **Claire D. Song**[1], **Jephrey Y. Liu**[7], **Giorgos C. Karakousis**[8], **Lynn M. Schuchter**[7], **Yiling Lu**[9], **Gordon Mills**[9], **Yusheng Cong**[11], **Jonathan Chernoff**[12], **Jun Guo**[13], **Genevieve M. Boland**[14], **Ryan J. Sullivan**[4], **Zhi Wei**[6], **Jeffrey Field**[10], **Ravi K. Amaravadi**[8], **Keith T. Flaherty**[4], **Meenhard Herlyn**[3,*], **Xiaowei Xu**[2,*], and **Wei Guo**[1,*]

[1]Department of Biology, the Hospital of the University of Pennsylvania, and Department of Dermatology, Perelman School of Medicine, University of Pennsylvania.

[2]Department of Pathology and Laboratory Medicine, the Hospital of the University of Pennsylvania, and Department of Dermatology, Perelman School of Medicine, University of Pennsylvania.

[3]Molecular and Cellular Oncogenesis Program and Melanoma Research Center, The Wistar Institute, Philadelphia, PA19104, U.S.A.

[4]Massachusetts General Hospital Cancer Center, Boston, MA02114, U.S.A.

[5]Department of Biology, Drexel University, Philadelphia, PA19104, U.S.A.

[6]Department of Computer Science, New Jersey Institute of Technology, Newark, NJ07102, U.S.A.

[7]Abramson Cancer Center and Department of Medicine, Perelman School of Medicine, University of Pennsylvania, Philadelphia, PA 19104, U.S.A.

[8]Department of Surgery, Hospital of the University of Pennsylvania, Philadelphia, PA19104, U.S.A.

[*]Send correspondence to: Wei Guo (guowei@sas.upenn.edu), Xiaowei Xu (xug@mail.med.upenn.edu) and Meenhard Herlyn (herlynm@wistar.org).

[15]These authors contributed equally to this work

SUPPLEMENTARY INFORMATION

Methods, along with additional Extended Data display items and Source Data, are available in the online version of the paper; references unique to these sections appear only in the online paper.

AUTHOR CONTRIBUTIONS

H.L, W.G. X.X., and M.H. conceived the project and designed and interpreted experiments. S.L., Y.Z., X.L. performed all the mice experiments. H.L. performed all Giemsa staining and IF staining; H.L. and S.L. performed all MTT assays; H.L., Y.Z., B.W., W.Z., W. Z., G. C., J.Z. performed Western blotting; G.Z., H.L. and S.L. performed FACS; G.Z., J.L., C.D.S., S.R., N.S., L.W.W., C.K., K.S., M.X. Y.C. and J.G. performed IHC staining and qPCR. Y.H., C.C., J.Z., and Z.W. performed bioinformatics and statistical analyses. Y.L. and G.M. performed the RPPA experiments. D.T.F., B.M., R.J.S., W.X., J.Y.L., G.C.K., L.M.S., G.M. B., J.C., J.F., R.K. A. and K.T. F. provided melanoma specimens, key constructs or associated clinical data. H.L. Z.G. and W.G. wrote the manuscript.

The authors declare no conflict of interests.

[9]Department of Systems Biology, The University of Texas MD Anderson Cancer Center, Houston, TX77054, USA.

[10]Department of Systems Pharmacology and Translational Therapeutics, Perelman School of Medicine, University of Pennsylvania, Philadelphia, PA19104, U.S.A.

[11]Institute of Aging Research, Hangzhou Normal University School of Medicine, Hangzhou, China.

[12]Cancer Biology Program, Fox Chase Cancer Center, Philadelphia, PA19111, U.S.A.

[13]Department of Renal Cancer and Melanoma, Peking University Cancer Hospital & Institute, Beijing, 100036, China.

[14]Department of Surgical Oncology, Massachusetts General Hospital, Boston, Massachusetts 02114, U.S.A.

Abstract

Targeted BRAF inhibition (BRAFi) and combined BRAF and MEK inhibition (BRAFi+MEKi) therapies have significantly improved clinical outcomes in patients with metastatic melanoma. Unfortunately, the efficacy is beset by the acquisition of drug resistance[1–6]. Here we investigated molecular mechanisms underlying acquired resistance to BRAFi (BRAFi resistance, “BR”) and BRAFi+MEKi (combination therapy resistance, “CR”). Consistent with previous studies, BR is mediated by ERK pathway re-activation. CR is, however, mediated by mechanisms independent of re-activation of ERK in many therapy-resistant cell lines and clinical samples. p21-activated kinases (PAKs) become activated in acquired drug resistant cells and play a pivotal role in mediating both BR and CR. Our screening using reverse phase protein array (RPPA) revealed distinct mechanisms by which PAKs mediate BR and CR. In BR, PAKs phosphorylate CRAF and MEK to reactivate ERK. In CR, PAKs regulate JNK and β-catenin phosphorylation, mTOR pathway activation, and inhibit apoptosis, thereby bypassing ERK. Together, our results provide new insights into molecular mechanisms underlying acquired drug resistance to current targeted therapies, and may help to direct novel drug development efforts to overcome acquired drug resistance.

Several mechanisms, including ERK re-activation[7,8], up-regulation of the mTOR[9] and WNT/β-catenin pathways[10], and modulation of apoptosis[11] have been reported to mediate acquired drug resistance to BRAFi. However, the molecular mechanisms underlying resistance to BRAFi+MEKi combination therapy, which is currently a standard approach for treating patients with BRAF-mutated melanoma, remain elusive.

In some patients, CR is mediated through mutations that augment mechanisms of BR, which activates downstream effectors of MAPK and PI3K signaling axes[5,12,13]. We examined the phosphorylation of ERK (“p-ERK$^{T202/Y204}$”) in both BR and CR cell lines. Consistent with previous findings, our immunoblotting analysis and immunohistochemistry (IHC) staining showed that the level of p-ERK$^{T202/Y204}$ was either similar to, or higher than, that of their respective parental cells in BR cells (Fig. 1a; Extended Data Fig. 1a)[2,14]. In CR, however, p-ERK$^{T202/Y204}$ was significantly reduced in 5 out of 6 cell lines compared to their respective parental cell lines (Fig. 1b). This observation was further corroborated by the IHC staining

of p-ERK$^{T202/Y204}$ in paired pre- and post-treatment tumor biopsy specimens from eight patients on BRAFi+MEKi therapy. p-ERK$^{T202/Y204}$ was elevated in 1 out of 8 post-treatment tumor biopsy specimens, but reduced or remained low for the rest (Fig. 1c, Extended Data Fig. 1b and Supplementary Table 1 and 2). We also analyzed p-ERK activity in BRAFi+MEKi resistant patient derived xenografts (CRPDX) tumor samples from four different mice, ERK was not reactivated when the mice were treated with BRAFi+MEKi (Extended Data Fig. 1c). The data suggest that the mechanisms underlying CR are different from those for BR in many patients.

We detected elevated levels of phospho-CRAF (p-CRAF^{S338}) in most of the acquired drug resistant cell lines, similar to previous studies[13] (Fig 1d and 1e). CRAF is directly phosphorylated by PAKs at Ser338[15,16]; we found that PAKs were activated in most of the resistant cells and CRPDX tumor samples (Fig. 1d and 1e; Extend Data Fig. 1c and 1d). PAKs are serine/threonine protein kinases that function downstream of small GTPases CDC42 and RAC1, and are involved in many tumorigenic pathways[17]. CDC42 and RAC1 show increased expression in some BR and CR cells (Extended Data Fig. 1e). qRT-PCR analysis show that the expression of *PAK1, PAK2, RAC1* and *CDC42* was elevated in post-treatment tumor biopsies derived from 8 patients with metastatic melanoma treated with either BRAFi or BRAFi+MEKi (Fig. 1f). In addition, gene set enrichment analysis of RNA-seq data derived from 6 patients' paired pre- and post-treatment tumor biopsy specimens and the public database[5,18] showed PAK signaling activation in most of tumor biopsies with acquired resistance to MAPK inhibitors (Extended Data Fig. 1f–1k and Supplementary Table 3).

It was previously reported that *BRAF^{V600E}* parental melanoma cells are insensitive to the inhibition of PAKs[19]. Here we found that, unlike parental cells, both BR and CR cells became sensitive to the PAK inhibitor PF-3758309[20] (Fig. 2a, Extended Data Fig. 2 and 3). FACS analyses showed that PAK inhibition retarded cell cycle progression with more cells arrested in $G_{0/1}$ phase (Extended Data Fig. 4). We also inhibited PAK1 function by RNAi knockdown, expression of the kinase-dead mutant of PAK1 (*PAK1^{K299R}*) and the PAK auto-inhibitory domain (*PAK1^{PID}*), or adding the inhibitor IPA-3. All of these approaches led to suppression of the viability of BR and CR cells (Fig. 2b, Extended Data Fig. 5a–5f; Supplementary Table 4). Conversely, ectopic expression of the constitutively active mutant of *PAK1* (*PAK1$^{107F/423E}$*) conferred drug resistance on 1205Lu parental cells to MAPK inhibitors (Fig. 2c). In addition to targeting PAK1, RNAi silencing of PAK4, a member of the Group II PAKs, also inhibited the growth of BR and CR cells (Extended Data Fig. 5g–5i). In mice, WM4008-1 (CRPDX) and other BR and CR cell lines tumor xenografts were sensitive to PAK inhibition (Fig. 2d and Extended Data Fig. 6), suggesting that PAKs play a critical role in the survival of therapy-resistant melanoma when the MAPK pathway is blocked.

PAKs are able to activate ERK by directly phosphorylating CRAF at Ser338 and MEK at Ser298[15,16]. We found that both p-CRAF^{Ser338} and p-MEK^{Ser298} were significantly increased in BR cells (Fig. 3a), and PF-3758309 down-regulated MAPK signaling in BR cell lines (Fig. 3b) and 1205Lu-BR xenograft (Fig. 3c). To gain a comprehensive understanding of signaling pathways that were altered in BR cell lines upon PAK inhibition, we treated 6

BR cell lines and 3 PDX-BR cell lines with PF-3758309 and profiled them using RPPA (Fig. 3d and Extended Data Fig. 7a). Several major changes were detected upon PF-3758309 treatment: (1) inhibition of the MAPK pathway as evidenced by the decrease in p-ERK$^{T202/Y204}$ and its downstream target p-c-Jun^{S73}; (2) inhibition of cell cycle progression as evidenced by the decrease in FOXM1, Cyclin B1 and CDK1, concurrent with the decrease in p-Rb$^{S807/811}$; (3) inhibition of mTOR signaling as evidenced by the decrease in p-S6$^{S235/S236}$, p-S6$^{S240/S244}$, p-4E-BP1^{S65} and p-4E-BP1$^{ST37/T46}$. We also examined the effect of expressing constitutively active *PAK1* in 1205Lu parental cell line using RPPA and immunoblotting. *PAK1*$^{107F/423E}$ had limited effect on cells in the absence of PLX4720, but blunted the inhibitory effect of PLX4720 on p-MEK1$^{S217/S221}$, p-ERK$^{T202/Y204}$, p-S6$^{S235/S236}$ and p-S6$^{S240/S244}$ (Fig. 3e and 3f).

For CR cells, PF-3758309 did not significantly affect the phosphorylation of ERK as observed in BR cells, but inhibited the ERK downstream p-ELK1^{S383} and RSK$^{T359/S363}$. In addition, mTOR pathway activity was mostly inhibited as indicated by the decrease in p-4E-BP1 and p-S6 (Fig. 4 and Extended Data Fig. 7b and 7c). Expression of the active *PAK1*$^{107F/423E}$ in 1205Lu parental cells did not lead to ERK re-activation in response to PLX4720 and PD0325901, but instead promoted cell cycle progression as suggested by the increase in p-Rb and p-cyclin B1. Furthermore, apoptosis was inhibited as indicated by the decrease in Bim and Bax in cells expressing constitutively active PAK1 (Extended Data Fig. 7d). Together, our analyses showed that PAKs mediate CR through at least three pathways. (1) PAK activation is required for sustained JNK activity. As JNK and ERK have common downstream targets such as ELK1, c-Jun and c-fos[21,22], JNK activity may partially compensate for the lack of ERK activation. (2) Activated PAKs and CRAF phosphorylate Bad, which blocks apoptotic signaling[17,23]. (3) PAKs regulate the phosphorylation of β-catenin. (4) PAKs probably activate the mTOR pathway[24] (Fig. 4a, b; Extended Data Fig. 7). Compared with parental and BR cells, CR cells were sensitive to JNK and S6K inhibitors, but less responsive to ERK inhibitor, consistent with a recent study[13] (Extended Data Fig. 8a and 8b). Similarly, silencing JNK and β-catenin by shRNA inhibits CR cell viability (Extended Data Fig. 8c–8e).

Our study reveals new mechanisms underlying acquired drug resistance to both BRAFi and BRAFi+MEKi therapies, and provides a comprehensive view of the re-wiring of the signaling networks in BR and CR cells (Extended Data Fig. 8f). The study highlights PAKs as pivotal mediators of drug resistance, and potential therapeutic targets for treating patients whose tumors progress on targeted therapies.

METHODS

Cell Culture, reagents, plasmids and antibodies

All human metastatic melanoma cell lines were established at The Wistar Institute as previously described[25]. They were authenticated by DNA fingerprinting and were tested regularly to avoid mycoplasma contamination before the assays. All of the melanoma cells were cultured in RPMI medium 1640 (Invitrogen, Inc.) supplemented with 5% FBS. Resistant cells were maintained with PLX4720 at 3μM for BR cells and RPDX cells or the combination of PLX4720 at 3μM plus PD0325901 at 300nM for CR cells throughout the

experiments. 1205Lu cells stably expressing the vector control or *PAK1*$^{L107F/T423E}$ mutant were selected using 1μg/ml puromycin for 10 days. DNA and RNA transfection were conducted using Lipofectamine 2000 (Invitrogen, Inc.), Fugene 6 (Roche, Inc.) or Lipofectamine RNAiMAX (Invitrogen, Inc.). The human *PAK1* siRNA sequence was 5'-GAAGAAATATACACGGTTT-3'; the *PAK2* siRNA sequence was 5'-AGAAGGAACTGATCATTAA-3'[26] and the control *LUCIFERASE GL2* siRNA sequence was 5'-AACGTACGCGGAATACTTCGA-3'. The shRNA targeting *JNK1, JNK1/2* and *B-CATENIN* were kindly provided by Drs. Stelios Andreadis (University of Buffalo) and Zhimin Lu (M.D. Anderson)[27–29]. The shRNA clones targeting *PAK4* were ordered from Sigma: 5'-GAGCCACAGCGAGTATCCCAT-3', 5'-CGAGAATGTGGTGGAGATGTA-3' and 5'-GACTCGATCCTGCTGACCCAT-3'.

PLX4720 and PD0325901 were provided by Plexxikon. PF-3758309 was provided by Pfizer. MEK162, LGX818, GSK2118436, GSK1120212, GDC0973 and PLX4032 were purchased from Selleckchem. Human kinase-dead *PAK1*^{K299R}, *PAK1*^{PID} mutant and constitutively active *PAK1*$^{L107F/T423E}$ mutant were cloned into the pCMV6 or pBabe PURO vector. All constructs were confirmed by sequencing. All information about the primary antibodies was included in Supplementary Table 5. Secondary antibodies were purchased from Invitrogen or GE Healthcare.

RNA extraction and real-time PCR

Total RNA was extracted using Trizol Reagent (Invitrogen, Inc.) according to the manufacturer's instruction. cDNA synthesis was performed with M-MLV reverse Transcriptase Kit (Promega, Inc.). Real-time PCR was performed using the Fast SYBR Green Master Mix Kit (Life Technologies). Amplifications were performed using an Applied Biosystems 7500 Real-Time PCR System (Life Technologies). All experiments were performed in triplicate. Expression ratios of controls were normalized to 1. Oligonucleotide primers used in RT-PCR: *PAK1*: GCTGTTCTGGATGTGTTGGA and TTCTGAAACTGGTGGCACTG; *PAK2*: ACAGAAGCACCCGCAGTAGT and AAAGACTTGGCAGCACCATC; *PAK4*: CAGGGAAGGCAGGCAGCCGA and CCTGTCACCACTGCCGCCAC; *RAC1*: CAATGCGTTCCCTGGAGAGTACA and ACGTCTGTTTGCGGGTAGGAGAG; *CDC42*: TAACTCACCACTGTCCAAAGACTCC and CCTCATCAAACACATTCTTCAGACC; GAPDH: GAAGGTGAAGGTCGGAGTC and GAAGATGGTGATGGGATTTC.

Cell viability, cell cycle and apoptosis assay

Cell viability was analyzed by Giemsa staining. Briefly, equal numbers of cells were seeded at approximately 40% confluency in 6-well plates and treated with DMSO or indicated inhibitors. The cells were then washed by PBS and fixed with methanol and acetone (1:1), and stained with Giemsa solution (Millipore) for 30 min. Cell density was measured by Image J. The values after background subtraction were normalized to the control group. MTT assay was performed using Cell Proliferation Kit I (Roche, Inc.) according to the manufacturer's instruction. The IC50 values were calculated from dose-response curves using Graphpad Prism 5.

For the apoptosis assay, BR and CR cells were treated with DMSO or PF3758309 for 72 hr. Cells were resuspended in 0.1ml PBS after centrifugation, and then co-stained with propidium iodide (Sigma) at 1 μg/ml and PSVue 643 (Molecular Targeting Technologies, Inc.) at 5μM. Cell suspensions were kept in dark at room temperature for 5 min. 0.2 ml PBS with 10% FBS was added to each cell suspension, and the cells were immediately analyzed by BD LSRII. For the cell cycle analysis, BR and CR cells were treated with DMSO or 1μM PF3758309 for 48 hr. Control or treated cells were fixed with ice cold 100% EtOH for 20 minutes, stained with propidium iodide and subsequently analyzed using a FACSCalibur. FSC and SSC gating was used to select single cells for the cell cycle analysis. The G_0/G_1 peak was centered at the PI/FL-2H Channel=200 using cells that were within the specified FL2-A/FLW gate. FCS files were then analyzed post-collection using ModFit software. Events that were in both the FSC/SSC and within the FL-2A/ FL-2W gates were analyzed to determine the percentage of cells in each stage of the cell cycle (PI/FL-2H).

Reverse phase protein array (RPPA)

The RPPA assay was performed by the MD Anderson Cancer Center core facility using 50 μg protein per sample. Antibodies were validated by Western blotting[30]. The RPPA data have been submitted to the Gene Expression Omnibus public database at the National Center for Biotechnology Information, following the information about RPPA experiment guidelines. The accession codes are GSE96902 and GSE96753.

IHC staining

IHC staining was performed on formalin-fixed, paraffin-embedded sections. Antigen retrieval was performed by steaming the slides in citrate buffer for 5 min (pH=6.0). Sections were incubated with anti-phospho-ERK (1:100; Cell Signaling, Inc.) antibody overnight at 4°C, followed by incubation with a biotinylated secondary antibody (1:200; Jackson Immuno Research) for 30 min. Detection was performed using Nova Red (Fisher Scientific, Inc.). The pathologist who examined the tumor was blinded to the clinical treatment information. There were no identifiable images of human research participants.

Patient specimen collection and generation of PDXs

Clinical data and tissue collection from patients with Stage IV melanoma was performed with informed consent at the University of Pennsylvania Abramson Cancer Center or Massachusetts General Hospital, in accordance with the Institutional Review Boards of both institutions. Data collection was performed in compliance with all relevant ethical regulations for human research participants. The collection of tumor tissues for the generation of PDXs was approved by the University of Pennsylvania Institutional Review Board[31]. PDX tumors derived from patients with metastatic melanoma who progressed on the combinatorial targeted therapies were expanded *in vivo* using NSG mice prior to the therapy experiments. The expansion phase was under the continuous drug pressure at approximately the clinical plasma levels.

Xenograft tumor model

The animal experiments were approved by Institutional Animal Care and Use Committee (IACUC) of the University of Pennsylvania and The Wistar Institute. Drug-resistant cells (5×10^6 cells per animal) were injected into flanks of 8-week-old female athymic *nu/nu* mice, and then allocated randomly to each treatment group. Daily oral administration of PLX4720 (200ppm), PD0325901 (7ppm) and PF-3758309 (25 ppm), individually or in combination, was started when the tumor volume in mice reached ~100 mm^3. Tumor volume was calculated using the formula: "Tumor volume = Length × Width × Width/2". They were subject to continued treatment until tumor reached 10% of the body weight or reached tumor dimension limit. For single tumors, growth was limited to a diameter of 2.0 cm (or the volume of 4.2 cm^3) at the widest point as long as the rodent remains healthy. For multiple tumors in a mouse, tumor growth was limited to a total diameter of 3.0 cm (the limit on any of the single tumor is still 2.0 cm). Throughout the experiments, all of the mice were carefully monitored at least twice a week for signs of distress, and were sacrificed when they were in poor body condition scores. Mice that died or with tumor sizes reached the dimension limit set by Penn IACUC guideline shortly after the start of the procedure were excluded from statistical analysis.

Statistical analyses and reproducibility

RPPA data analysis was performed according to the protocol from the M.D. Anderson Cancer Center. Specifically, relative protein levels for each sample were determined by interpolation of each dilution curves from the "standard curve" (supercurve) of the slide (antibody). Supercurve is constructed by a script in R written by the RPPA core facility. These values are defined as Supercurve Log2 value. All the data points were normalized for protein loading and transformed to linear value, designated as "Normalized Linear". "Normalized Linear" value was transformed to Log2 value, and then median-centered for further analysis. Median-Centered values were centered by subtracting the median of all samples in a given protein. All of the above-mentioned procedures were performed by the RPPA core facility. The normalized data provided by the RPPA core facility were analyzed via the LIMMA package in R. For Extended Data Fig. 7a, we presented the proteins showing significant changes (false discovery rate is controlled at 0.01 level by using the Benjamini-Hochberg procedure for multiple comparison correction) in at least 4 BR cell lines out of the 9 BR cell lines after PF3758309 treatment versus DMSO. Similarly, for Extended Data Fig. 7b, we presented the proteins showing significant changes in at least 2 CR cell lines out the 3 CR cell lines after PF3758309 treatment versus DMSO.

The microarray data were analyzed with the lumi package in the R/Bioconductor environment[32]. The probes were filtered to include genes with a detection P value <0.05 in all samples for use in further analyses. The data was transformed by a Variance-Stabilizing Transformation (VST) and then normalized by a Quantile Normalization using the lumi package. The microarray data of genes of interest including *PAKs, RAC1* and *CDC42* were extracted and were visualized in heat maps using heat map.2 program within the gplots package for R.

The enrichment score (Extended Data Fig. 1g, 1i and 1k) was done with single sample GSEA (ssGSEA) method[33], and was carried out using GSVApackage in R[34]. The Enrichment Score (ES) in ssGSEA method essentially is the weighted sum of the difference between the empirical cumulative distribution functions of the genes within the gene signature and the remaining genes.

All other statistical analyses were performed using software R, version 2.14. Two-way ANOVA (mouse tumor volumes) and log-rank test (mouse survival) were used to compare data between PLX4720 or PLX4720 with PD0325901 and all other groups, no multiple comparisons. Two-side student's test was used for pairwise comparison for the remaining datasets.

DATA AVAILABILITY STATEMENT

RPPA data are available at NCBI under accession numbers GSE96902 and GSE96753. Patient information is provided in Supplementary Table 1. Information for p-ERK IHC staining is provided in Supplementary Table 2. Information for patients with PAK pathway activation is provided in Supplementary Table 3. IC50 values for MTT assays are provided in Supplementary Table 4. Antibody information is provided in Supplementary Table 5. All mouse data are provided in Supplementary Table 6. The number of times for the experiments completed independently with similar results is list in the Supplemental Table 7. For immunoblot Source Data, see Supplementary Fig. 1. Source Data are provided for all graphs. All of the data are available from the authors upon reasonable request.

Extended Data

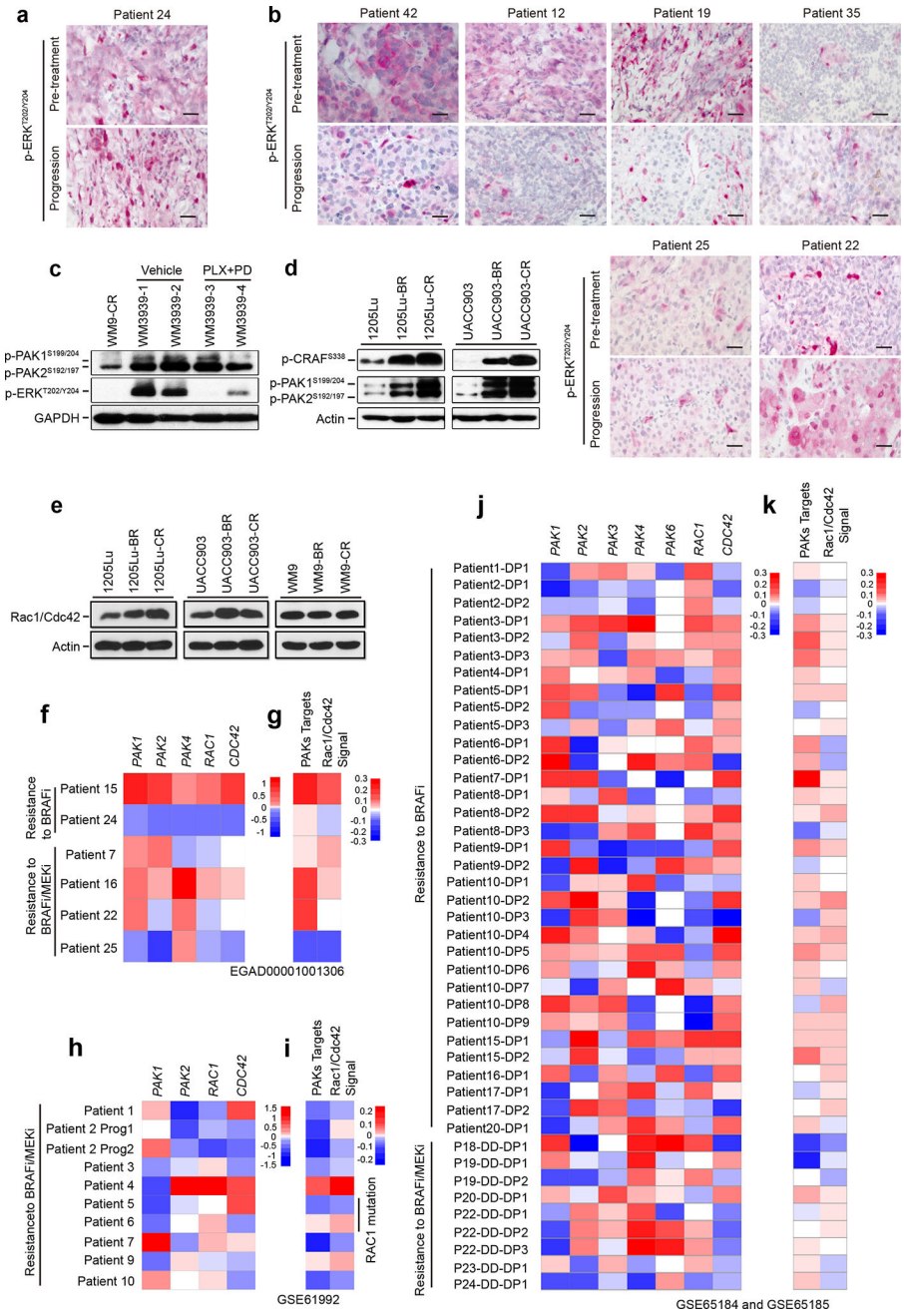

Extended Data Figure 1. ERK and PAK activity in BRAFi and BRAFi+MEKi resistance melanoma. Related to Figure 1

a and **b.** IHC staining of p-ERK$^{T202/Y204}$ in paired pre- and post-treatment tumor biopsy specimens procured from patients who relapsed on BRAFi (**a**) or BRAFi+MEKi (**b**). Note that some of the strongly positive-stained cells are macrophages rather than tumor cells. Scale bar, 50 μm. The tissues were stained with Nova Red. **c.** Western blotting analysis showed the levels of p-ERK$^{T202/Y204}$ and p-PAK1$^{S199/204}$/PAK2$^{S192/197}$ in WM3939 PDX-CR tumor samples. Tumors from mice treated with vehicle control, or with BRAFi+MEKi

were shown. WM9-CR was used for comparison. **d.** Western blotting of PAK phosphorylation in matching parental, BR and CR cells. **e.** Western blotting using a polyclonal antibody that recognizes both Cdc42 and Rac1 in matching parental, BR and CR cells. Cdc42 and Rac1 could not be separated by SDS-PAGE due to their similar molecular weights. **f, h** and **j.** Heatmaps of expression levels of *PAKs, RAC1* and *CDC42* in paired pre- and post-treatment tumor biopsy specimens procured from patients with metastatic melanoma who progressed on MAPK inhibitors. Data were analyzed using LIMMA package in R. The fold change of expression levels in paired post-treatment tumor biopsy specimen over pre-treatment tumor biopsy specimen was shown in the heatmap. Color scale, log2 transformed expression for each gene was normalized to the mean value of all samples. **g, i** and **k.** Heatmaps of the enrichment scores of two PAK signaling-related gene sets in paired pre- and post-treatment tumor biopsy specimens procured from patients with metastatic melanoma who relapsed on MAPK inhibitors. The value for each entry is the difference of enrichment score from post-treatment over pre-treatment specimens. Gene expression microarray or RNA-seq data were downloaded from EGAD00001001306, GSE65184, GSE65185 and GSE61992.

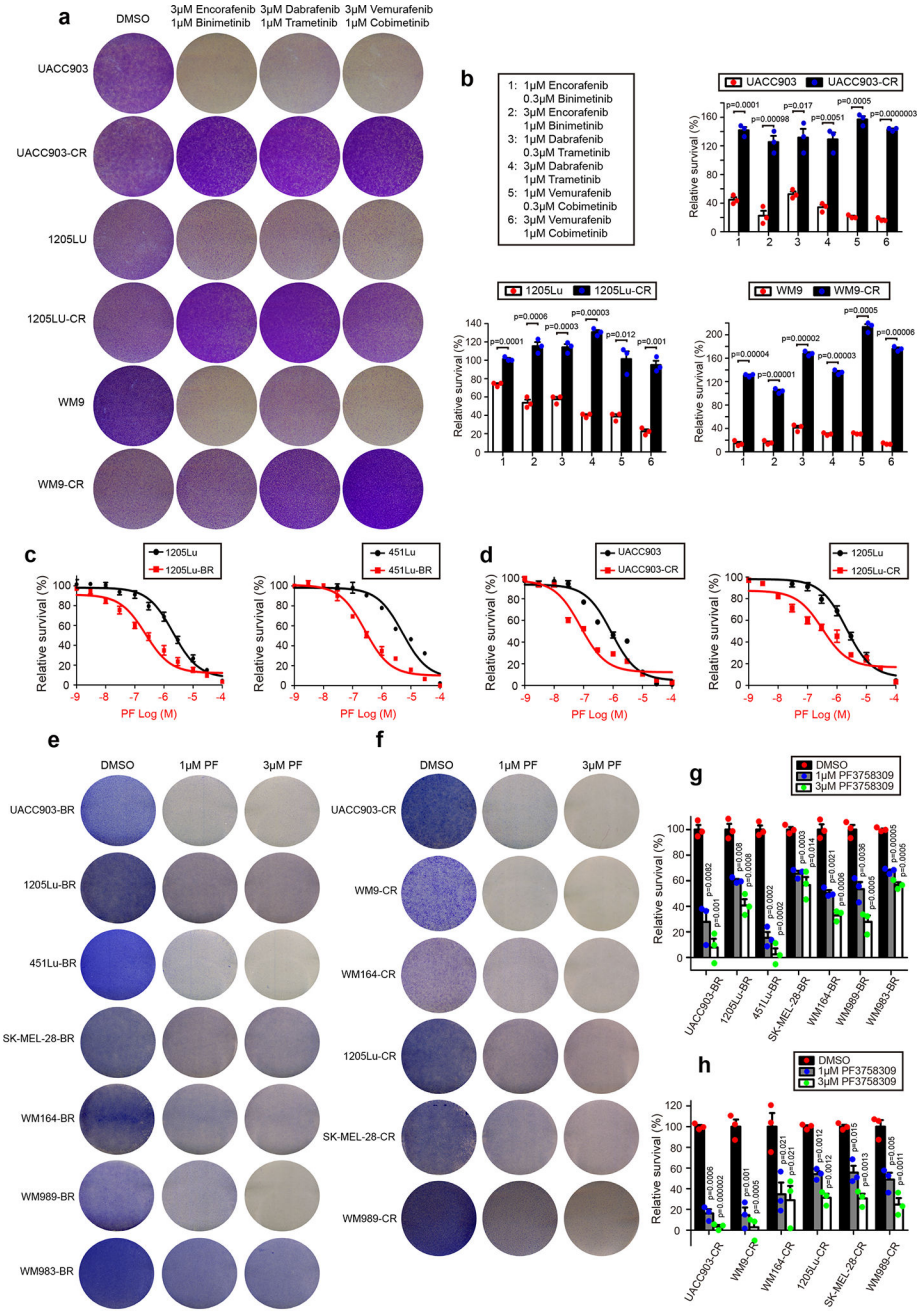

Extended Data Figure 2. CR cells resistant to the combination of PLX4720 and PD0325901 exhibit cross-resistance to other combinations of BRAF and MEK inhibitors, and are sensitive to PAK inhibitor PF-3758309. Related to Figure 2

a. Paired parental and CR cells were treated with the combination of three different sets of BRAF and MEK inhibitors, separately, for 4 days and then fixed and stained with Giemsa. **b.** Quantification of cell survival (n=3 biologically independent samples). **c** and **d**, Relative survival of matching parental, BR and CR cells treated with increasing concentrations of PF-3758309 (n=3 or 4 biologically independent samples, as indicated in the figure). All IC50 values were list in Supplementary Table 4. Two-sided Student's t-test was used for statistical analyses of the IC50 values. **e–h.** 7 BR (**e**) and 6 CR cell lines (**f**) were treated

with DMSO, 1μM or 3μM PF3758309 for 72 hr, and then fixed and stained with Giemsa. The data were quantified in (**g**) for BR and (**h**) CR cells (n=3 biologically independent samples). Cell density was measured by Image J. The values after background subtraction were normalized to parental cells treated with DMSO. Two-sided Student's t-test was used for statistical analyses (**b, c, d, g** and **h**); Data are plotted as mean ± SEM.

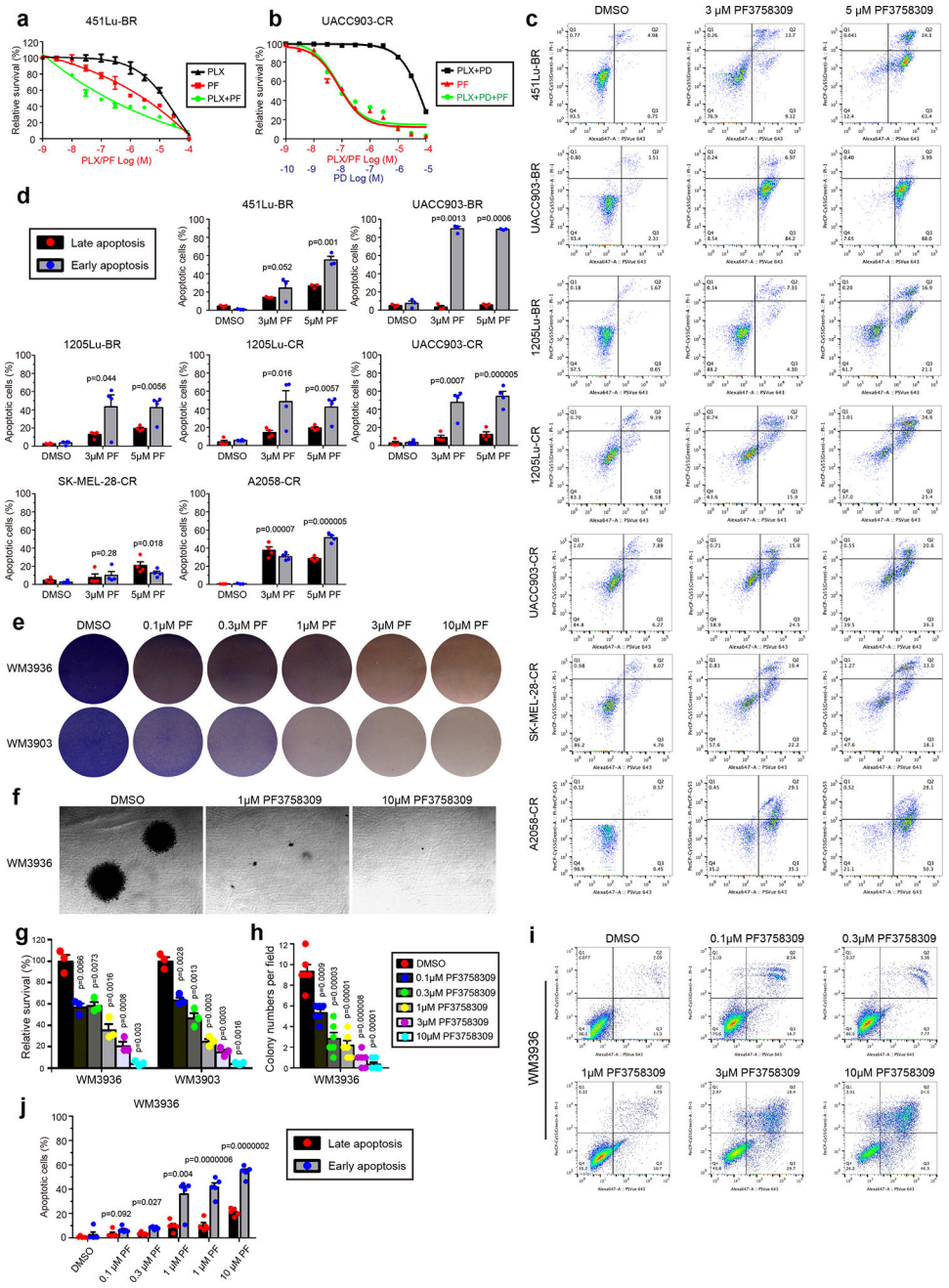

Extended Data Figure 3. Inhibition of PAKs by PF3758309 decreased the viability of drug resistant melanoma cells. Related to Figure 2

a and **b.** Relative survival of BR and CR cells treated with increasing concentrations of the PF-3758309 ("PF"), PLX4720 ("PLX"), and PD0325901 ("PD") for 48 hr. Cell viability

was analyzed by MTT assay. The data were normalized to cells treated with DMSO (n=4 biologically independent samples). **c.** FACS analysis of BR cells and CR cells treated with PF3758309. All the cells were labeled with propidium iodide and PSVue 643, and then analyzed by BD LSRII. **d.** Quantification of cell apoptosis. The percentage of apoptosis cells after PF3758309 treatment was compared with the cells treated with DMSO (n=3 or 4 biologically independent samples as indicated in the figure). **e.** Giemsa staining of the PDX-BR cells WM3936 and WM3903 that were treated with DMSO, or different concentrations of PF3758309 for 3 days. The staining was quantified in **(g)** (n=3 biologically independent samples). **f.** Anchorage independent growth assay of WM3936 cells. A total of 2000 cells were seeded in medium with soft agar in six-well plates. Scale bar, 200μm. The number of colonies in each field was quantified in **(h)** (n=6 biologically independent samples). **i.** WM3936 cells were treated with DMSO or different concentrations of PF3758309 for 3 days. All cells were labeled with propidium iodide and PSVue 643, and then analyzed by BD LSRII. **j.** Quantification of cell apoptosis. The percentage of apoptosis cells after PF3758309 treatment was compared with the cells treated with DMSO (n=5 biologically independent samples). Two-sided Student's t-test (**a, b, d, g, h** and **j**) was used for statistical analyses. Data are plotted as mean ± SEM.

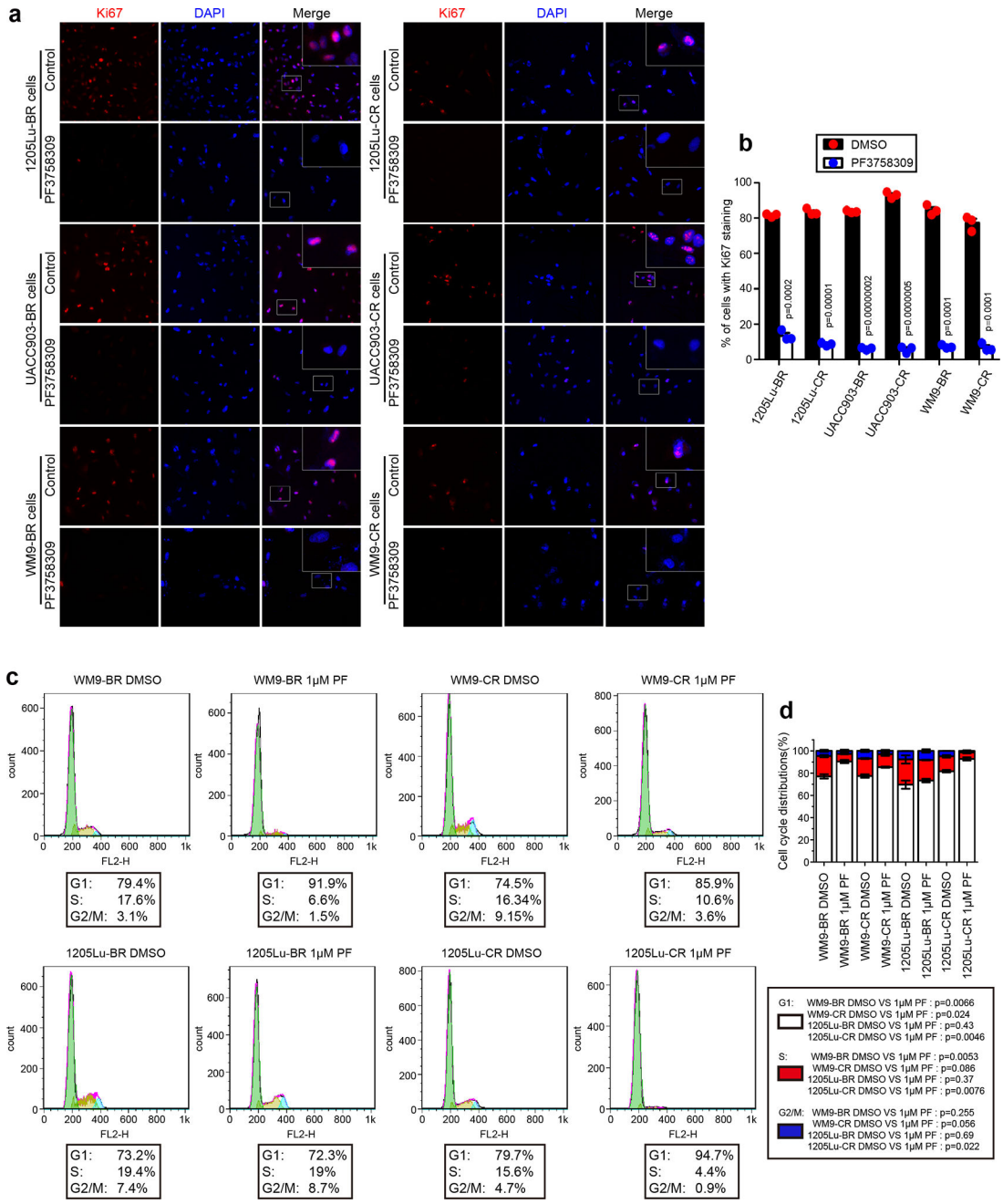

Extended Data Figure 4. Cell cycle analysis of BR and CR cells treated with PF3758309. Related to Figure 2

a. Immunofluorescence staining of Ki67 (red) in indicated cells, which were treated with DMSO or 1μM PF3758309. The nuclei were stained with DAPI (blue). **b.** Quantification of cells with Ki67 staining (n>70 cells/ per assay, 3 independent experiments). **c.** Flow cytometric analysis (10000 cells were analyzed per assay). Cells were fixed, stained with PI, and then analyzed by a FACscan flow cytometer and ModFit LT (Verity Software) **d.** Histograms of PI staining (n=3 biologically independent samples). Two-sided Student's t-test (**b** and **d**) was used for statistical analyses. Data are plotted as mean ± SEM.

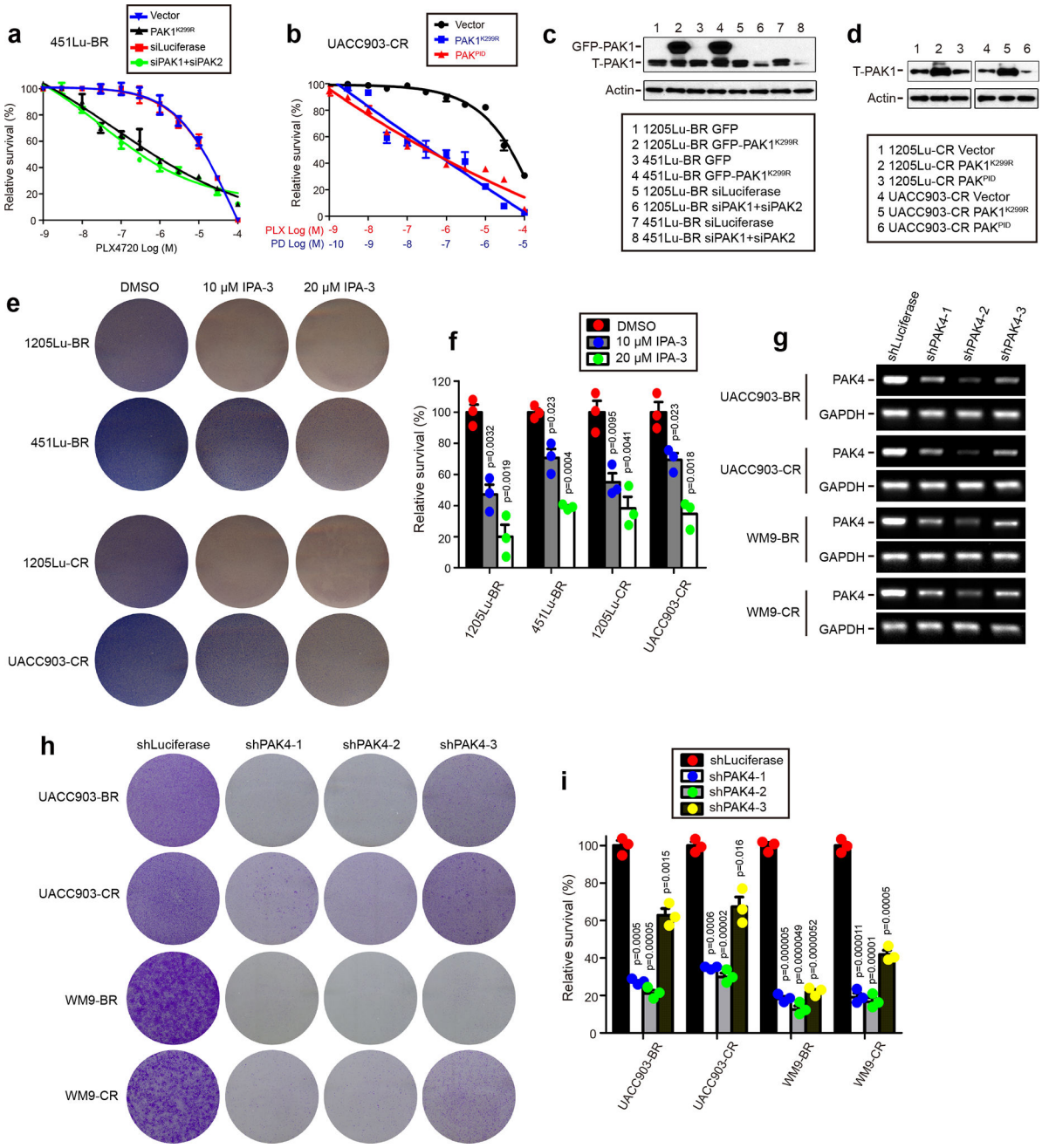

Extended Data Figure 5. Inhibition of PAKs by siRNA, kinase-dead dominant-negative *PAK1*^{K299R} mutant or PAK inhibitor IPA-3 decreased the viability of drug resistant melanoma cells. Related to Figure 2

a and **b.** Relative survival of BR or CR cells transfected with PAK1^{K299R} or PAK1^{PID}, or siRNA against PAK1 and PAK2. Cells were then cultured with PLX4720 or PLX4720+PD0325901 at different concentrations for 48 hr. Cell viability was analyzed by MTT assays (n=4 biologically independent samples). Two-sided Student's t-test (for IC50 values) was used for statistical analysis. **c** and **d.** PAK1 and actin levels in cells were analyzed by Western blotting. **e.** BR and CR cells were treated with DMSO, 10μM or 20μM IPA-3 for 72 hr, and then processed for Giemsa staining. **f**. Quantification of the staining in

(e) (n=3 biologically independent samples). **g.** RT-PCR analysis of the expression of *PAK4* in indicated cells. **h.** Giemsa staining of indicated cells. **i.** Quantification of the staining in **(h)** (n=3 biologically independent samples). Two-sided Student's t-test (**a, b, f** and **i**) was used for statistical analysis. Data are plotted as mean ± SEM.

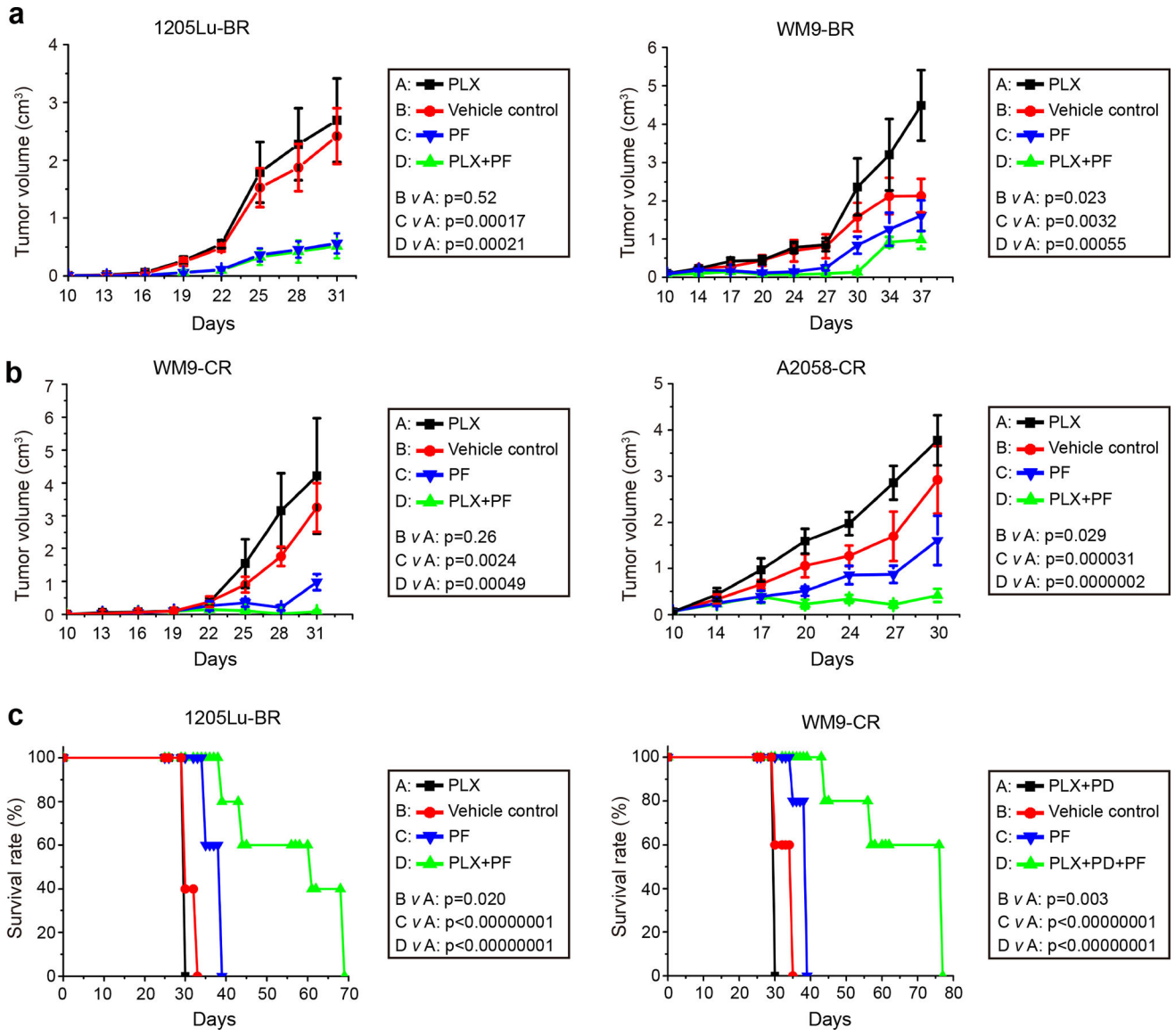

Extended Data Figure 6. Combined inhibition of MAPK and PAK pathways significantly inhibited BR and CR tumor proliferation in mice and improved survival. Related to Figure 2

a and **b.** Tumor growth curves. Mice were injected with 1205Lu-BR (n=9 mice per group) or WM9-BR (n=9 mice per group) (**a**), WM9-CR (n=5 mice per group) or A2058-CR cells (control n=8, other n=9 mice per group) (**b**), and proceed for MAPK or PAK inhibition for indicated days. **c**. Survival curves of the mice bearing 1205Lu-BR and WM9-CR xenografts. (n=5 mice per group). All groups were compared with the PLX or PLX+PD group; no multiple comparisons. Two-way ANOVA (**a** and **b**) and log-rank test (**c**) was used for statistical analyses. Individual tumor volume data points can be found in the Source Data.

Data are plotted as mean ± SEM. For mouse survival, the function survdiff from the survival R package was used.

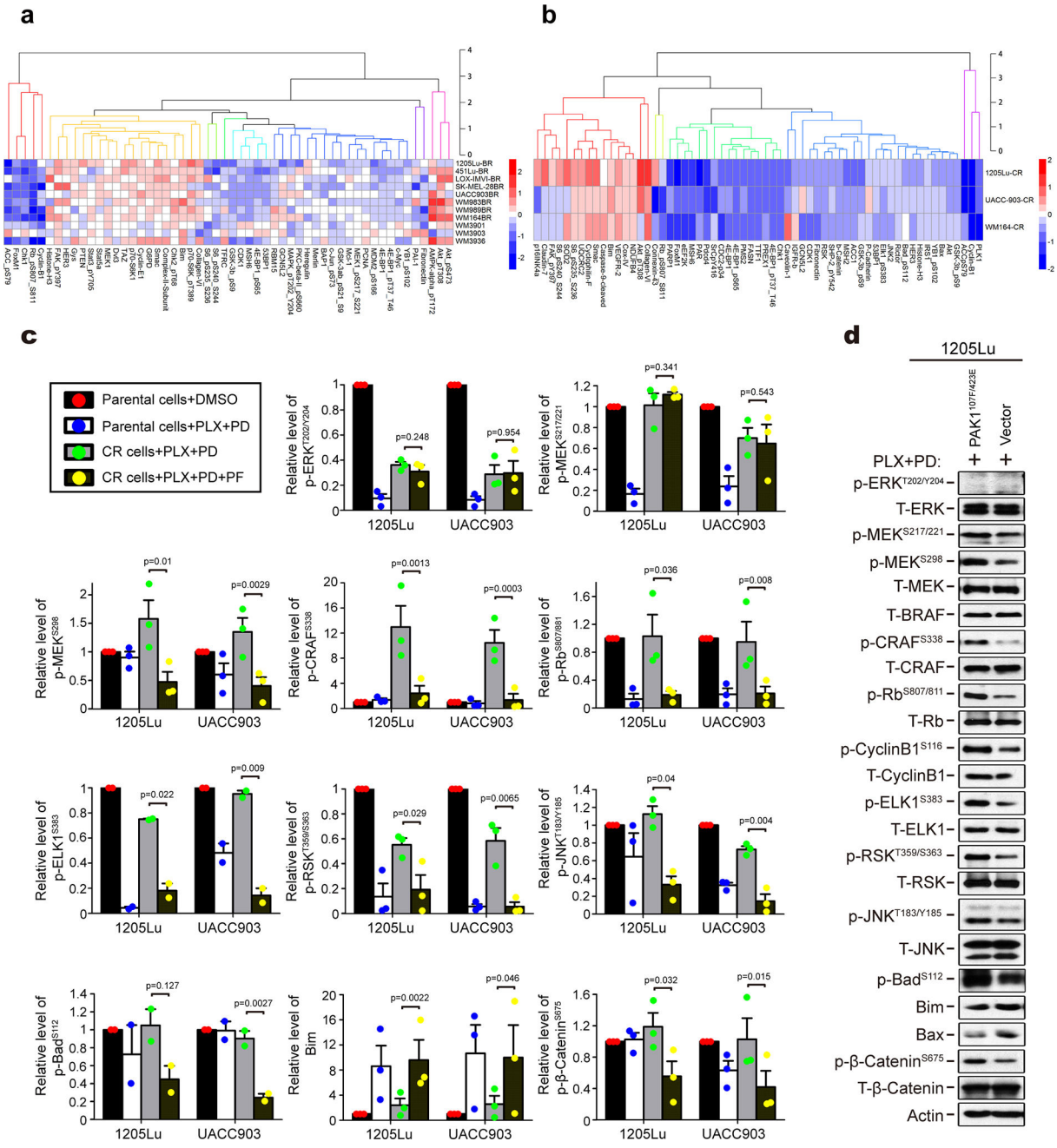

Extended Data Figure 7. RPPA and immunoblotting analyses of signaling proteins in melanoma cells treated with MAPK inhibitor or PAK inhibitor. Related to Figure 3 and 4

a. 8 BR cell lines and 3 PDX-BR cell lines were treated with DMSO or PF3758309 for 48 hr. Protein lysates from these cells were then analyzed by RPPA. Data were analyzed using LIMMA package in R. The levels of identified proteins (that displayed significant changes in at least 4 BR cell lines after PF3758309 treatment versus DMSO, P <0.01) were shown in the heat map. Color scale, log2 transformed expression for each protein was normalized to

the mean value of all samples. **b.** 1205Lu-CR, UACC903-CR and WM164-CR cells were treated with DMSO or PF3758309 for 48 hr. Cell lysates were analyzed by RPPA. Data were analyzed using LIMMA package in R. The levels of identified proteins (that displayed significant changes in at least 2 CR cell lines after PF3758309 treatment versus DMSO, P <0.01) were shown in the heatmap. Color scale, log2 transformed expression (Red, high; Blue, low) for each protein was normalized to the mean value of all samples. **c.** 1205Lu and UACC903 parental and CR cells were treated as indicated (**Figure 4b**). Protein levels were analyzed in three independent assays, and the staining was measured by Image J. (n=2 for p-ELK1^{S383} and p-Bad^{S112}, n=3 for all other proteins). To minimize variations caused by different exposure time in each independent assay, the staining was normalized to the mean of all the samples from its group before statistical analyses. Two-sided Student's t-test. Data are plotted as mean ± SEM. **d.** 1205Lu cells stably expressing *PAK1*$^{107F/423E}$ or vector control were treated with 1μM PLX4720 and 100nM PD0325901 for 48 hr. The levels of MAPK pathway-related proteins, cell cycle-related proteins and apoptosis-related proteins were analyzed by Western blotting.

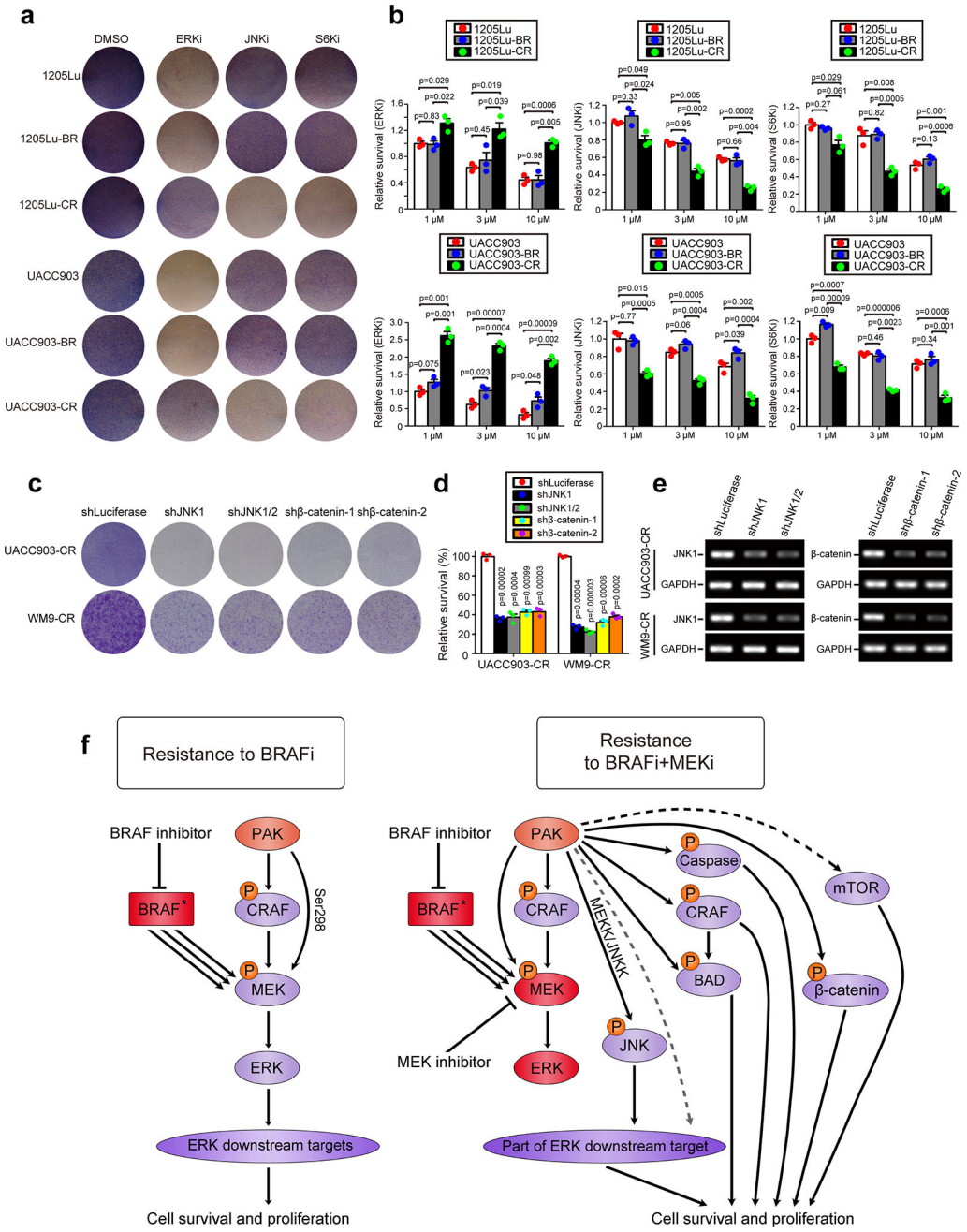

Extended Data Figure 8. Inhibition of JNK, S6K or β-catenin inhibited BR and CR cell viability. Related to Figure 4

a. Giemsa staining of 1205Lu and UACC903 parental, BR and CR cells that were treated with either DMSO, the ERK inhibitor SCH772984 (3 μM), the JNK inhibitor SP600125 (3 μM) or the S6K inhibitor PF-4708671 (3 μM) for 3 days. **b**. Quantification of cell survival (n=3 biologically independent samples). Cell density was quantified with Image J. The values were normalized to those of parental cells treated with 1μM respective inhibitor. **c.** Giemsa staining of indicated cells that were infected with Luciferase shRNA, JNK1 shRNA, JNK1/2 shRNA and two different β-catenin shRNA. The staining was quantified in **(d)** (n=3

biologically independent samples). **e.** RT-PCR analysis of the expression of JNK1 and β-catenin in indicated cells. **f.** Schematic diagrams showing the molecular mechanisms by which PAKs mediate acquired drug resistance of $BRAF^{V600E}$ melanoma cells to BRAFi (the left panel) and BRAFi+MEKi (the right panel). For data presented in this figure, two-sided Student's t-test (**b** and **d**) was used for statistical analyses. Data are plotted as mean ± SEM.

Supplementary Material

Refer to Web version on PubMed Central for supplementary material.

Acknowledgments

We thank Pfizer, Inc. for providing PF-3758309, and Plexxikon, Inc. for providing PLX4720 and PD0325901. This work is supported by NIH grants R01-GM085146, U54-CA193417 and CA174523 pilot grant to W.G., CA114046, CA25874 and CA174523 to X.X., and the Dr. Miriam and Sheldon G. Adelson Medical Research Foundation and NCI CA025874, CA114046 and CA174523 to M.H.

References

1. Chapman PB, et al. Improved survival with vemurafenib in melanoma with BRAF V600E mutation. N. Engl. J. Med. 2011; 364:2507–2516. [PubMed: 21639808]
2. Shi H, et al. Acquired resistance and clonal evolution in melanoma during BRAF inhibitor therapy. Cancer Discov. 2014; 4:80–93. [PubMed: 24265155]
3. Boussemart L, et al. eIF4F is a nexus of resistance to anti-BRAF and anti-MEK cancer therapies. Nature. 2014; 513:105–109. [PubMed: 25079330]
4. Larkin J, et al. Combined vemurafenib and cobimetinib in BRAF-mutated melanoma. N. Engl. J. Med. 2014; 371:1867–1876. [PubMed: 25265494]
5. Long GV, et al. Increased MAPK reactivation in early resistance to dabrafenib/trametinib combination therapy of BRAF-mutant metastatic melanoma. Nat. Commun. 2014; 5:5694. [PubMed: 25452114]
6. Long GV, et al. Combined BRAF and MEK inhibition versus BRAF inhibition alone in melanoma. N. Engl. J. Med. 2014; 371:1877–1888. [PubMed: 25265492]
7. Nazarian R, et al. Melanomas acquire resistance to B-RAF(V600E) inhibition by RTK or N-RAS upregulation. Nature. 2010; 468:973–977. [PubMed: 21107323]
8. Johannessen CM, et al. A melanocyte lineage program confers resistance to MAP kinase pathway inhibition. Nature. 2013; 504:138–142. [PubMed: 24185007]
9. Villanueva J, et al. Acquired resistance to BRAF inhibitors mediated by a RAF kinase switch in melanoma can be overcome by cotargeting MEK and IGF-1R/PI3K. Cancer Cell. 2010; 18:683–695. [PubMed: 21156289]
10. Anastas JN, et al. WNT5A enhances resistance of melanoma cells to targeted BRAF inhibitors. J. Clin. Invest. 2014; 124:2877–2890. [PubMed: 24865425]
11. Tentori L, Lacal PM, Graziani G. Challenging resistance mechanisms to therapies for metastatic melanoma. Trends Pharmacol. Sci. 2013; 34:656–666. [PubMed: 24210882]
12. Wagle N, et al. MAP kinase pathway alterations in BRAF-mutant melanoma patients with acquired resistance to combined RAF/MEK inhibition. Cancer Discov. 2014; 4:61–68. [PubMed: 24265154]
13. Moriceau G, et al. Tunable-combinatorial mechanisms of acquired resistance limit the efficacy of BRAF/MEK cotargeting but result in melanoma drug addiction. Cancer Cell. 2015; 27:240–256. [PubMed: 25600339]
14. Van Allen EM, et al. The genetic landscape of clinical resistance to RAF inhibition in metastatic melanoma. Cancer Discov. 2014; 4:94–109. [PubMed: 24265153]
15. King AJ, et al. The protein kinase Pak3 positively regulates Raf-1 activity through phosphorylation of serine 338. Nature. 1998; 396:180–183. [PubMed: 9823899]

16. Tran NH, Frost JA. Phosphorylation of Raf-1 by p21-activated kinase 1 and Src regulates Raf-1 autoinhibition. J. Biol. Chem. 2003; 278:11221–11226. [PubMed: 12551923]
17. Radu M, Semenova G, Kosoff R, Chernoff J. PAK signalling during the development and progression of cancer. Nature Rev. Cancer. 2014; 14:13–25. [PubMed: 24505617]
18. Hugo W, et al. Non-genomic and Immune Evolution of Melanoma Acquiring MAPKi Resistance. Cell. 2015; 162:1271–1285. [PubMed: 26359985]
19. Ong CC, et al. P21-activated kinase 1 (PAK1) as a therapeutic target in BRAF wild-type melanoma. J. Natl. Cancer Inst. 2013; 105:606–607. [PubMed: 23535073]
20. Murray BW, et al. Small-molecule p21-activated kinase inhibitor PF-3758309 is a potent inhibitor of oncogenic signaling and tumor growth. Proc. Natl Acad. Sci. USA. 2010; 107:9446–9451. [PubMed: 20439741]
21. Cavigelli M, Dolfi F, Claret FX, Karin M. Induction of c-fos expression through JNK-mediated TCF/Elk-1 phosphorylation. EMBO J. 1995; 14:5957–5964. [PubMed: 8846788]
22. Bagrodia S, Derijard B, Davis RJ, Cerione RA. Cdc42 and PAK-mediated signaling leads to Jun kinase and p38 mitogen-activated protein kinase activation. J. Biol. Chem. 1995; 270:27995–27998. [PubMed: 7499279]
23. Alavi A, Hood JD, Frausto R, Stupack DG, Cheresh DA. Role of Raf in vascular protection from distinct apoptotic stimuli. Science. 2003; 301:94–96. [PubMed: 12843393]
24. Higuchi M, Onishi K, Kikuchi C, Gotoh Y. Scaffolding function of PAK in the PDK1-Akt pathway. Nature Cell Bio. 2008; 10:1356–1364. [PubMed: 18931661]
25. Zhang G, et al. Targeting mitochondrial biogenesis to overcome drug resistance to MAPK inhibitors. J Clin Invest. 2016; 126:1834–1856. [PubMed: 27043285]
26. Coniglio SJ, Zavarella S, Symons MH. Pak1 and Pak2 mediate tumor cell invasion through distinct signaling mechanisms. Mol. Cell. Biol. 2008; 28:4162–4172. [PubMed: 18411304]
27. Arias-Romero LE, Villamar-Cruz O, Huang M, Hoeflich KP, Chernoff J. Pak1 kinase links ErbB2 to beta-catenin in transformation of breast epithelial cells. Cancer Res. 2013; 73:3671–3682. [PubMed: 23576562]
28. You H, et al. JNK regulates compliance-induced adherens junctions formation in epithelial cells and tissues. J. Cell Sci. 2013; 126:2718–2729. [PubMed: 23591817]
29. Ji H, Wang J, Fang B, Fang X, Lu Z. alpha-Catenin inhibits glioma cell migration, invasion, and proliferation by suppression of beta-catenin transactivation. J. Neurooncol. 2011; 103:445–451. [PubMed: 20872274]
30. Tibes R, et al. Reverse phase protein array: validation of a novel proteomic technology and utility for analysis of primary leukemia specimens and hematopoietic stem cells. Mol. Cancer Ther. 2006; 5:2512–2521. [PubMed: 17041095]
31. Krepler C, et al. Personalized Preclinical Trials in BRAF Inhibitor-Resistant Patient-Derived Xenograft Models Identify Second-Line Combination Therapies. Clin. Cancer Res. 2016; 22:1592–1602. [PubMed: 26673799]
32. Nazarian R, et al. Melanomas acquire resistance to B-RAF(V600E) inhibition by RTK or N-RAS upregulation. Nature. 2010; 468:973–977. [PubMed: 21107323]
33. Barbie DA, Tamayo P, Boehm JS, Kim SY, Moody SE, et al. Systematic RNA interference reveals that oncogenic KRAS-driven cancers require TBK1. Nature. 2009; 462:108–112. [PubMed: 19847166]
34. Hänzelmann S, Castelo R, Guinney J. GSVA: gene set variation analysis for microarray and RNA-Seq data. BMC Bioinformatics. 2013; 14

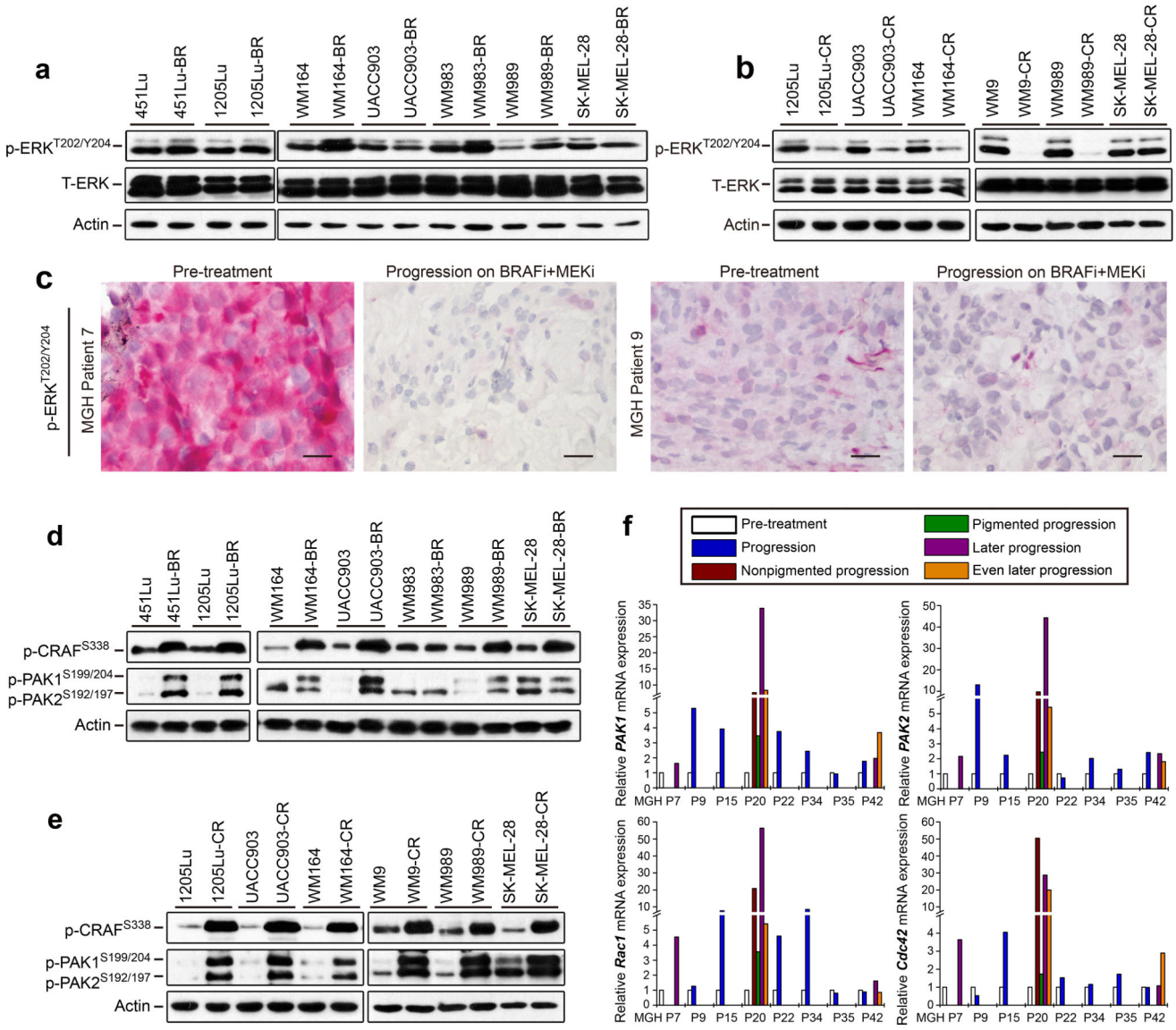

Figure 1. Activation of PAK signaling in *BRAF*^{V600E} melanoma cells with acquired drug resistance

a and **b.** Levels of ERK and phospho-ERK in paired parental and BR **(a)** and CR cells **(b). c.** IHC staining of paired pre- and post-BRAFi/MEKi tumor biopsies with anti-p-ERK antibody. Scale bar, 50μm. **d** and **e.** Immunoblotting analysis of phosphorylated CRAF and PAKs in paired parental and BR (**d**) and CR (**e**) cell lines. **f.** qRT-PCR analysis of *PAK1, PAK2, RAC1* and *CDC42* in paired pre- and post-treatment tumor biopsies derived from melanoma patients.

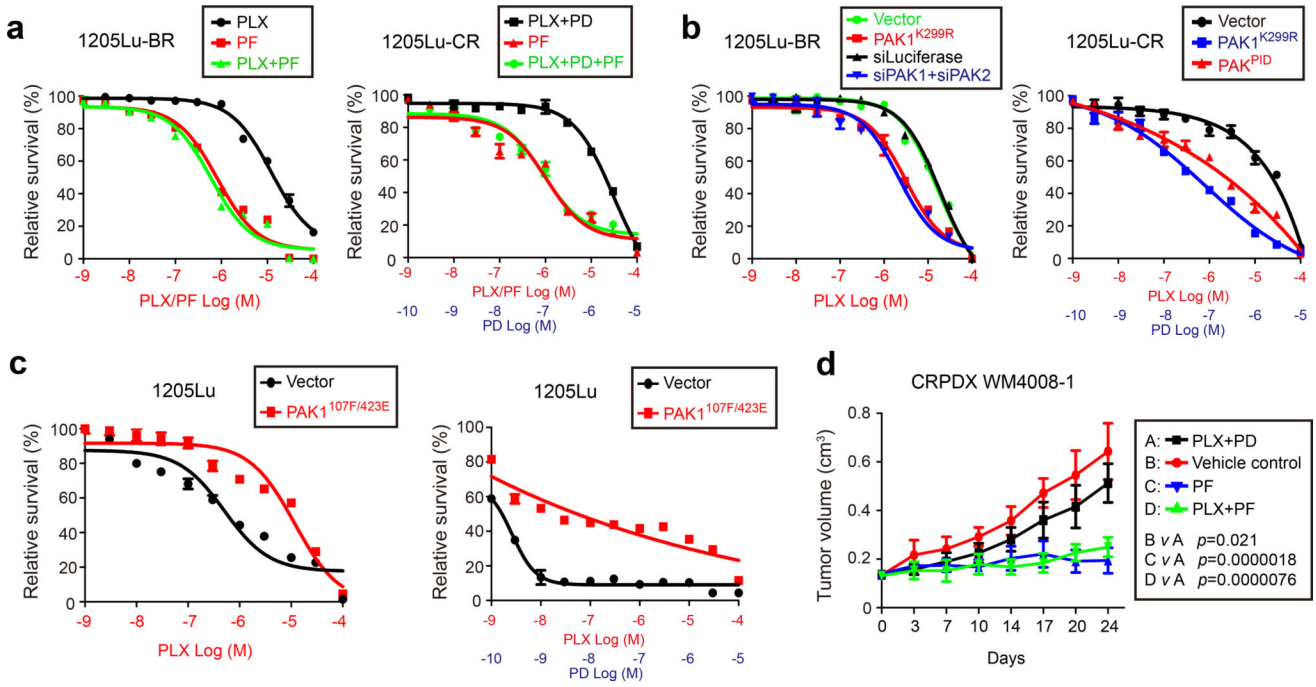

Figure 2. Inhibition of PAK activity overcomes acquired drug resistance

a, Relative survival of 1205Lu BR and CR cells treated with increasing concentrations of PF-3758309, PLX4720, and PD0325901. **b** and **c**, Relative survival of indicated cells transfected with *PAK1*^{K299R} or *PAK1*^{PID}, or siRNA against *PAK1* and *PAK2* (**b**) or *PAK1*$^{107F/423E}$ (**c**). Cells were cultured with PLX4720 or PLX4720+PD0325901 and analyzed by MTT. Data were normalized to control cells treated with DMSO (n=4 biologically independent samples). **d.** Tumor growth curves of WM4008-1 xenograft with indicated treatments (n=5 mice). For statistics, two-sided Student's t-test (IC50 values in **a–c**) and two-way ANOVA (**d**) were used. Data are plotted as mean ± SEM. Tumor volume data points can be found in the Source Data.

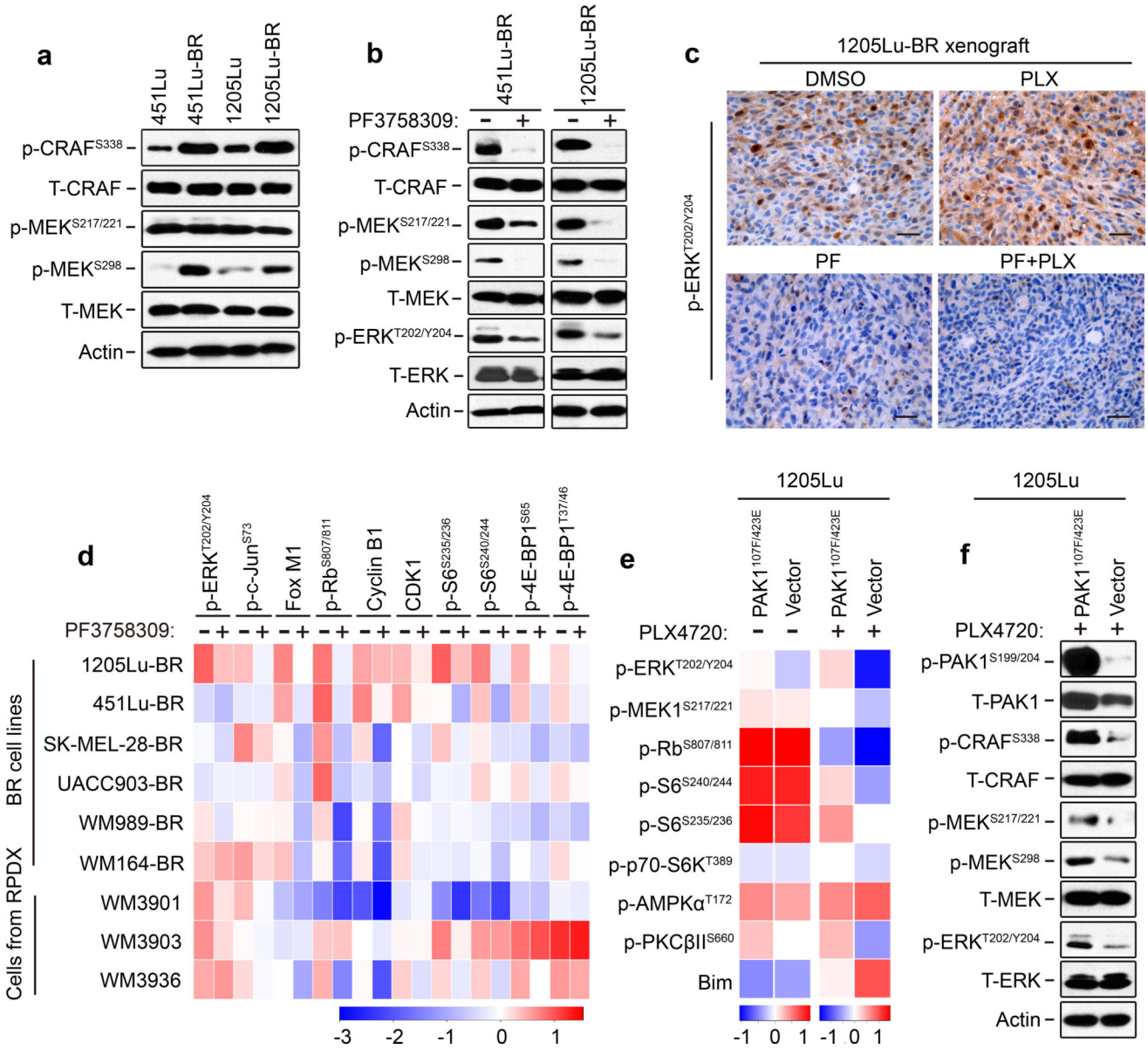

Figure 3. PAKs mediate the re-activation of ERK signaling in BR melanoma cells

a and **b**. Immunoblotting analysis of indicated signaling proteins in parental and BR cells (**a**) or BR cells treated with PF-3758309 (**b**). **c.** p-ERK IHC staining of 1205Lu-BR xenograft tumors treated with indicated inhibitors. Scale bar, 50μm. **d.** Heat map analysis of indicated proteins in BR cells treated with PF-3758309. **e.** Heat map analysis of indicated proteins in 1205Lu cells expressing *PAK1*$^{107F/423E}$ in the absence and presence of PLX4720. **f**. Immunoblotting analysis of indicated signaling proteins in cells stably expressing *PAK1*$^{107F/423E}$ treated with PLX4720.

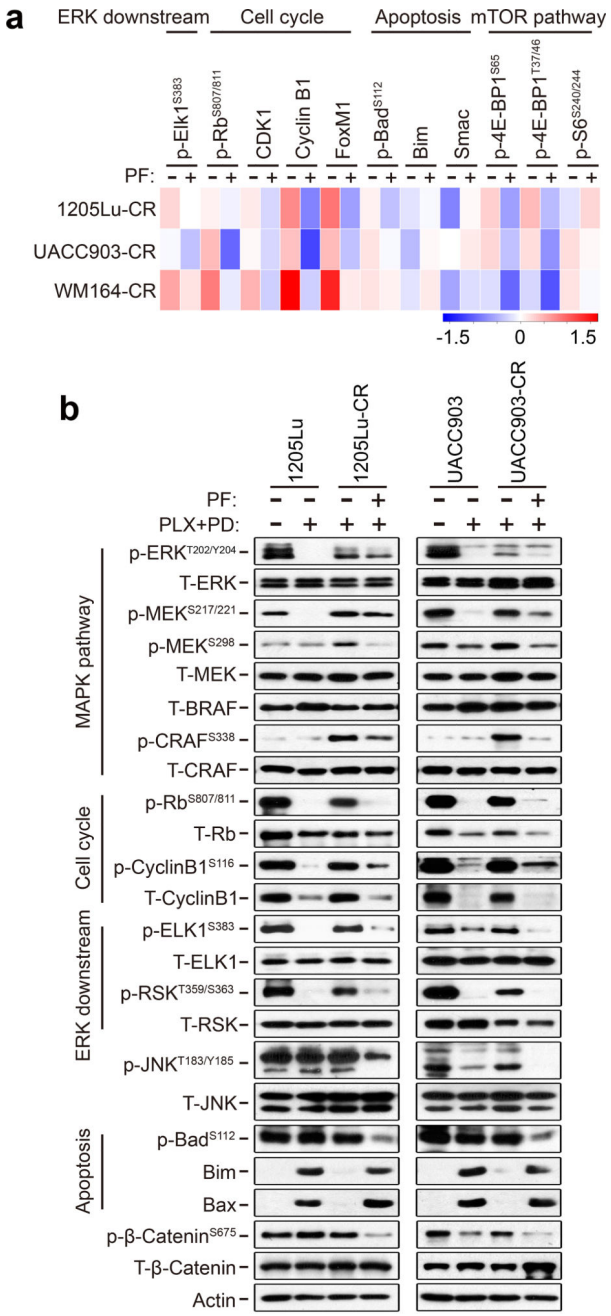

Figure 4. Signaling pathways in CR melanoma cells with PAK inhibition

a. Heat map analysis of indicated proteins in CR cells treated with PF-3758309. **b.** Immunoblotting analysis of 1205Lu and UACC903 parental and CR cells under indicated treatments. The levels of MAPK pathway-related proteins, cell cycle-related proteins and apoptosis-related proteins were analyzed.